Design and optimal integration of seasonal borehole thermal energy storage in district heating and cooling networks.

Massimo Fiorentini [a], *Jacopo* Vivian [a], *Philipp* Heer [a], *Luca* Baldini [b]

[a] Urban Energy Systems Laboratory, Empa - Swiss Federal Laboratories for Materials Science and Technology, 8600 Dübendorf, Switzerland.

[b] Centre for Building Technologies and Processes, ZHAW Zurich University of Applied Sciences, 8401 Winterthur, Switzerland.

Abstract. Technologies that can close the seasonal gap between summer renewable generation and winter heating demand are crucial in reducing CO_2 emissions of energy systems. Borehole thermal energy storage (BTES) systems offer an attractive solution, and their correct sizing is important for their techno-economic success. Most of the BTES design studies either employ detailed modelling and simulation techniques, which are not suitable for numerical optimization, or use significantly simplified models that do not consider the effects of operational variables. This paper proposes a BTES modelling approach and a mixed-integer bilinear programming formulation that can consider the influence of the seasonal BTES temperature swing on its capacity, thermal losses, maximum heat transfer rate and on the efficiency of connected heat pumps or chillers. This enables an accurate assessment of its integration performance in different district heating and cooling networks operated at different temperatures and with different operating modes (e.g. direct discharge of the BTES or via a heat pump). Considering a case study utilizing air sourced heat pumps under seasonally varying CO_2 intensity of the electricity, the optimal design and operation of an energy system integrating a BTES and solar thermal collectors were studied. The optimization, aiming at minimizing the annual cost and CO_2 emissions of the energy system, was applied to two heating network temperatures and five representative carbon prices. Results show that the optimal BTES design changed in terms of both size and operational conditions, and reductions in emissions up to 43% could be achieved compared to a standard air-source heat pumps based system.

Keywords. Renewable heating and cooling, seasonal thermal storage, borehole thermal energy storage (BTES), district heating/cooling networks, design optimization, optimal management.
DOI: https://doi.org/10.34641/clima.2022.64

1. Introduction

In the frame of the United Nations' climate conferences (COPs) and the declared target of limiting the atmospheric temperature, there is a strong need for fast decarbonization of our economies. This involves a substitution of fossil fuels with renewables, which due to their non-dispatchable nature, require a significant increase in storage capacity build-up in the energy system. Electric, thermal and chemical storages play a crucial role and all converge in their effect as the sectoral coupling is strengthened. In this context, coupling electric heat pumps with large scale seasonal thermal energy storage is essential for decarbonising heat and cold supply for buildings. Seasonal load shifting through thermal energy storage enables a strict minimization of total CO_2 emissions and thus supports moving away from the so far common *energy* efficiency perspective. Leveraging that, Borehole Thermal Energy Storage systems are an attractive solution. Historically, BTES systems were designed to support centralized solar plants and were designed to operate at high temperatures, such as the implementation in Drake Landing in Canada [1]. These installations show a BTES efficiency generally lower than expected at the design stage. This is one of the reasons that led modern systems to generally operate BTES at lower temperatures, reducing thermal losses but also enabling integration of waste heat sources at relatively low temperatures.

To this end, finding optimal combined design and operational strategies for these technologies is

important to ensure they achieve their techno-economical objectives.

BTESs are generally modelled in detail using software tools such as TRNSYS [2] at both district [3] and residential scales [4], but this approach does not allow the application of numerical optimization methods, requiring iterative processes to optimize the system configuration. The energy-hub approach, which is based on numerical optimization methods and employed in district heating and cooling system design, can help with this task. Nevertheless, only a few studies included seasonal thermal energy storage within their framework, particularly considering a BTES [5–7]. To formulate the system design optimization as a Mixed-Integer Linear Programming (MILP) problem, these studies do not model the dynamical behaviour of the thermal storage (temperature evolution, heat transfer mechanisms) influencing the storage properties and the efficiency of the connected equipment. The performance of a BTES is highly dependent on how it is used in relation to defined boundary conditions, as highlighted in [8]. Potential alternative approaches were proposed in [9], employing genetic algorithms to optimize non-linear models. An alternative approach, based on a mixed-integer bilinear optimization framework, is also proposed in a manuscript by some of the authors currently under review [10], and extended in this study. The bilinear problem formulation, a particular subcategory of non-linear problems, enables finding a guaranteed optimal solution using modern solvers such as Gurobi [11].

The proposed method, outlined in [10] and extended in this study, can consider: i) the influence of operational variables such as the initial temperature of the BTES and the storage temperature swing (seasonal sinusoidal fluctuation of the average BTES temperature) on the total capacity of the storage and thermal losses of the storage, ii) the relationship between the volume of the BTES and its maximum heat transfer rate and iii) the impact of boundary conditions such as the availability of solar thermal generation, the CO_2 intensity of the grid electricity consumed on the optimal design of the storage and energy system.

In particular, this paper studies an electricity-based heating and cooling system coupled with a BTES and investigates its optimal design considering the effect of different BTES parameters such as its size, its integration in networks operating at different temperatures and the possibility to discharge it either directly or through a heat-pump on the overall system performance and operational carbon dioxide emissions. The proposed optimization framework is employed to identify optimal system design (sizing and operation), including BTES, heat pumps, chillers and solar collectors, leading to optimal trade-offs between operational CO_2 emissions and levelized cost.

2. Energy system layout

In this paper, we study a generic district heating and cooling system with a centralized design, which has the possibility to integrate a BTES to store thermal energy seasonally. It is assumed that the BTES is cylindrical, with uniformly distributed boreholes and a parallel plumbing configuration. In line with the requirement of avoiding the use of fossil fuels for heat generation, it is assumed that the district's cooling demand can be met by two chillers, one that rejects the waste heat in a BTES and a second one that uses the ambient air as a sink. Similarly, the heating demand can be met by two heat pumps, also using the BTES and the ambient air as sources, together with the possibility to directly discharge the BTES when its temperature is higher than the district heating supply temperature. As the heating demand of the site might differ significantly from the cooling one, an additional solar thermal heat source can be considered in the design optimization of the system. The solar thermal system is assumed to be able to provide heat either directly to the district heating system, or store it in the BTES. It is also assumed that the solar thermal collectors are coupled with a buffer tank large enough to absorb daily fluctuations in energy generation. A schematic of the system is presented in Fig. 1.

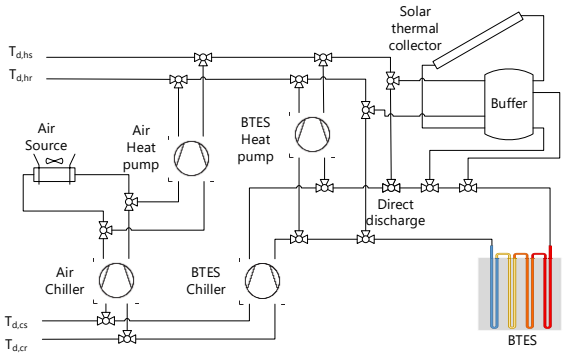

Fig. 1 - Case study centralized district heating and cooling system layout.

3. Methods

This Section presents the main inputs (3.1) and assumptions (3.4) used and a description of the optimization model, including the constraints (3.2) and the objective function (3.3).

3.1 Inputs and optimization framework

The optimization framework uses weather conditions (solar radiation I_t and ambient temperature T_a), a CO_2 intensity profile (I_{CO2}), and heating ($P_{load,heat}$) and cooling demand profiles ($P_{load,cool}$) as inputs. It returns the optimal system design in terms of technology sizing and operational conditions, listed below. The input data are provided with a daily resolution for a year, and they are assumed not to change along the lifetime of the system. It is assumed that the system must strictly meet the defined heating and cooling demand. The

decision variables include:

- The optimal equipment sizing, including the heat pump and chillers heating and cooling capacity (S_{hp_BT},S_{ch_BT},S_{hp_a},S_{ch_a}), solar thermal collectors area (S_{sol}), and the size (ground volume) of the BTES (discretized, V_j).
- The optimal initial temperature of the BTES ($T_{BT,init}$).
- The fraction of heating and cooling demand provided, by the solar generation (P_{th,sol_used}), by the direct discharge of the BTES (P_{th,BT_direct}), by the heat pump and chiller connected to the BTES (P_{th,hp_BT}, P_{th,ch_BT}) or by the air-source heat pump and chiller (P_{th,hp_a}, P_{th,ch_a}) at each time step *k*,
- The fraction of solar generation stored in the BTES (P_{th,sol_tr}) at each time step *k*.

The electrical power consumption of each heat pump ($P_{\mathrm{el,hp_{BT}}}$, $P_{\mathrm{el,hp_a}}$) and chiller ($P_{\mathrm{el,ch_{BT}}}$, $P_{\mathrm{el,ch_a}}$) is calculated at each time step *k* to derive the total energy system ($P_{el,tot}$), used to estimate the operational costs and CO_2 emissions to be included in the optimization objective function. Consumption of circulation pumps is considered negligible in this study, as the pumping energy difference among cases is small and not affected by operational conditions and temperatures as much as heat pumps and chillers.

3.2 Models and constraints

BTES

In this optimization framework, BTES sizing was discretized as the properties of the storage change with the storage volume, such as the thermal losses and the maximum heat transfer rate. The BTES is modelled as a single capacitance with losses calculated with the steady-state equation proposed by Hellström [12] as a function of the storage depth, storage aspect ratio and ground thermal conductivity. This model is considered valid as it is assumed that the BTES is cylindrical, with uniformly distributed boreholes, and employing an in-parallel plumbing setup. The top insulation, of area A_i and a U-value U_i, contributes to the losses. A number of n_j storage sizes are considered, each corresponding to a storage volume V_j. As it is assumed that the storage keeps the same aspect ratio (diameter equal to depth) when scaled, the heat loss factor h is the same for each size considered. The equation proposed by Hellström can also be employed to model storages with a parallelepipedal shape. Other shapes can be used in this optimization framework, as long as the temperature dynamics are described by a linear time-invariant model. The storage temperature evolution for the *j-th* size is presented in Eq. 1:

$$T_{BT}(k+1) = T_{BT}(k) + \frac{\Delta t}{\rho_g c_{p,g} V_j}\left(\left(P_{\mathrm{th,ch_{BT}}} + P_{\mathrm{el,ch_{BT}}}\right) + P_{\mathrm{th,sol_{tr}}} - \left(P_{\mathrm{th,hp_{BT}}} - P_{\mathrm{el,hp_{BT}}}\right) - P_{\mathrm{th,dir_{BT}}} - U_i A_{i,j}\left(T_{BT}(k) - T_a(k)\right) - k_g h \frac{D_j}{2}\left(T_{BT}(k) - T_g(k)\right)\right) \quad (1)$$

where T_{BT} is the temperature of the storage, T_a the ambient temperature, T_{sol} is the supply temperature of the solar system and T_g is the undisturbed ground temperature. ρ_g and $c_{p,g}$ are the density and specific heat capacity of the ground respectively. As direct charge and discharge with the heat pump must not occur simultaneously, a Boolean variable δ_m is introduced with (2) and (3) to define which operating mode is being used (in this case δ_m is equal to 1 when the heat pump is used) and constraining to zero the heat provided in the other mode. Furthermore, if the temperature of the storage T_{BT} is lower or equal to the network heating supply temperature $T_{d,hs}$, the BTES cannot be discharged directly (i.e. δ_m = 1). The supply temperature of the thermal network is not considered as a decision variable, but as a constant parameter. An equivalent UA_j coefficient is used to linearly represent the heat exchange in the boreholes and is calculated for each BTES size, assuming a uniform borehole wall temperature that is equal to the overall BTES temperature. In this study, the value of this UA coefficient was identified as presented in [8]. The heat transfer is constrained in each storage size by the total UA value (UA_j) of the ground heat exchangers and the temperature difference between heat transfer fluid and storage (ΔT_{eq}, T_{sol} - T_{BT}). An example of this constraint for rejection of heat from cooling operations is shown in Eq. 2:

$$P_{th\_ch_{BT}} \leq \delta_m (UA_j \Delta T_{eq} - P_{el_{ch_{BT}}}) \quad (2)$$

A similar constraint is applied to the direct discharge of the BTES as well, which is expressed as in Eq. 3.

$$P_{th\_dir_{BT}} \leq (1-\delta_m) UA_j \left(T_{BT} - T_{d,hr}\right) \quad (3)$$

The BTES cost (J_{BT}) in each scaling option is obtained from the total drilling length, calculated as the product of the number of ground heat exchangers ($n_{GHX,j}$) and their depth (D_j), multiplied by a drilling price per meter (λ_{GHX}) and an annuity factor (ω_{BT}), as presented in Eq. 4:

$$J_{BT} = D_j n_{GHX,j} \lambda_{GHX} \omega_{BT} \quad (4)$$

Several constraints are introduced in the optimization problem, which are not listed explicitly for conciseness. These ensure that: i) only one size of storage can be selected at a time, ii) that the storage temperature and the storage initial temperature are within predefined temperature boundaries, iii) that the storage temperature at the beginning and end of the year is the same.

Heat pumps and chillers

To enable the optimization to choose the best source between the BTES and the air sources for providing heating and cooling, the sizing and the operation of the two heat pumps and chillers are considered as optimization variables. The heating and cooling capacity of each energy conversion equipment is constrained between zero and the maximum heating demand of the plant. For instance, the heat pump

using the BTES as a source is presented in Eq. 5.

$$0 \leq S_{hp\_BT} \leq P_{th,load\_heat}^{max} \quad (5)$$

The COP of the air-source heat pump and chiller, as it is not a function of a state of the system and can be pre-computed before the optimization is performed. Indeed, the temperatures of district heating and cooling networks are constant, as explained in the BTES model subsection. An example for the air-source heat pump supplying heat to the district network at temperature $T_{d,hs}$ is calculated as in Eq. 6.

$$COP_{hp\_air}(k) = 0.5 \frac{T_{d,hs}}{T_{d,hs}-(T_a-\Delta T_{eq})} \quad (6)$$

As the COP of the heat pump and chiller connected to the BTES are a function of a state of the system (i.e. the temperature of the BTES), the following linearized relationship of the inverse of the COP was employed to calculate the electrical consumption of the equipment, as presented in Eq. 7.

$$COP_{hp_{BT}}^{-1}(k) = a_{hp}\left(T_{BT}(k) - \Delta T_{eq}\right) + b_{hp} \quad (7)$$

Solar collectors

To support the optimization with a daily resolution, it is assumed that the solar panels are coupled with a buffer tank capable of shifting part of the daily generation to the night. The collectors are also assumed to operate at a constant efficiency η_{sol}. The heat generation of the solar panels $P_{th,sol}$ can be calculated at each time step as in Eq. 8:

$$P_{th\_sol}(k) = \eta_{sol} I_{sol}(k) S_{sol} \quad (8)$$

where I_{sol} is the solar radiation and S_{sol} the solar array area. A constraint on the maximum size of the array is also added. The buffer tank is size S_{STTS} is designed to shift half of the maximum daily solar generation:

$$S_{STTS}(k) = \eta_{sol} I_{sol}^{max} S_{sol} \Delta t/2 \quad (9)$$

The solar energy can be either used directly for heating operations ($P_{th\_sol,used}$) or transferred to charge the BTES ($P_{th\_sol,transf}$), provided that the sum of these two elements, at each time step, does not exceed the total heat production $P_{th,sol}$.

Plant thermal balance

Thermal energy loads must be met at each time step, using the available energy resources. The heating load can be provided by the solar system directly, by the direct discharge of the BTES, as well as by the air-source and BTES heat pumps (Eq. 10).

$$P_{load,heat}(k) = P_{th\_hp_{BT}}(k) + P_{th\_hp_a}(k) + P_{th\_dir_{BT}}(k) + P_{th\_sol,used}(k) \quad (10)$$

Similarly, the cooling demand can be satisfied by the air source and BTES chillers (Eq. 11).

$$P_{load,cool}(k) = P_{th\_ch_{BT}}(k) + P_{th\_ch_a}(k) \quad (11)$$

3.3 Objective function

The objective of the optimization is to minimize the annual cost of the energy system, which comprises of three elements: i) a capital component (J_c), ii) an operational component associated with the electricity consumption ($J_{o,e}$) and iii) an operational component associated with the cost of CO_2 emissions ($J_{o,CO2}$). These are shown in Eq. 12, Eq. 13 and Eq. 14 respectively.

$$J_c = \omega_{eq}\left(\lambda_{hp}\left(S_{hp_{BT}} + S_{hp_a}\right) + \lambda_{ch}\left(S_{ch_{BT}} + S_{ch_a}\right) + \lambda_{sol} S_{sol} + \lambda_{STTS} S_{STTS}\right) \quad (12)$$

$$J_{o,e} = \sum_{k=1}^{N} (P_{el,tot}(k)) \nu_{el} \Delta t \quad (13)$$

$$J_{o,CO2} = \sum_{k=1}^{N} (I_{CO2}(k) P_{el,tot}(k)) \nu_{CO2} \Delta t \quad (14)$$

Maintenance costs are neglected in this formulation.

3.4 Implementation

The optimization problem was formulated in Matlab R2020b, using the YALMIP toolbox [13] and Gurobi v9.1 as a solver [11]. A maximum MIPGap 0f 0.1% was considered as a stopping criterion for each optimization run.

Heating and cooling demand

The heating and cooling demand data were collected from the operational history of the Empa campus in Dübendorf, Switzerland, which includes 35 buildings of different use (e.g. office, laboratory, etc.) thus requiring energy both for process and space heating and cooling. The thermal energy, currently generated with a natural gas boiler and a chiller, is distributed to the buildings using two separate thermal grids. The resulting net demand of the campus was calculated from an hourly dataset and averaged over each day, thus obtaining the daily load profiles shown in Fig. 2.

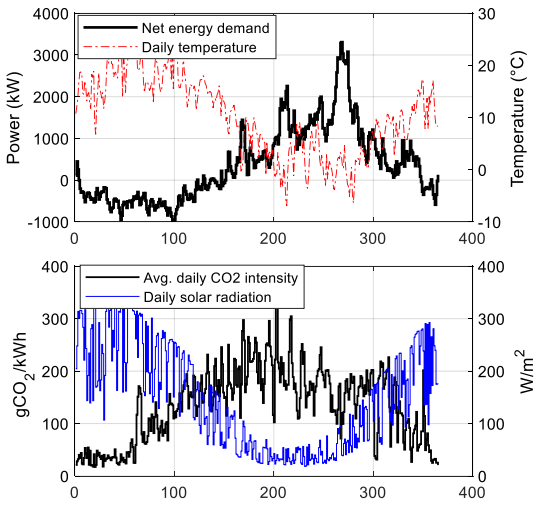

Fig. 2. Boundary conditions for the optimization: energy demand and outdoor temperature (top); CO_2

intensity and solar irradiation (bottom).

The peak heat demand was approximately 3.3 MW and the maximum cooling demand approximately 1 MW. The climate data were taken from the Dübendorf TMYx weather file [14]. The CO_2 equivalent intensity profile for Switzerland was sourced from [15].

Assumptions on techno-economic parameters

The size of the borehole thermal energy storage was selected among five volumes, all with the same cylindrical shape and aspect ratio (equal depth and diameter). Therefore, increasing the volume V of the storage results in an increase in both depth and diameter (D) and number of the boreholes (n_b), as shown in Table 1. The optimization can also choose not to include the BTES if this option minimizes the objective function shown in Section 3.3.

Tab. 1 – BTES design options.

Opt.	D (m)	V (10^3 m^3)	UA (kW/K)	n_b (-)
1	53.4	119.2	22.5	158
2	61.2	179.6	33.8	207
3	70.0	269.4	50.6	271
4	80.1	404.1	76.0	355
5	91.7	606.1	113.9	466
6	No BTES			

The undisturbed ground temperature and the thermal conductivity of the ground were assumed to be 12°C and 2.4 W/(m*K), respectively. The annual cost of the BTES was calculated assuming a lifetime of 60 years, and a borehole cost of 66 €/m [16]. This study does not consider the initial transient to reach a stable temperature swing, which can be problematic at a high initial storage temperature $T_{BT,0}$. Therefore, an upper limit on the initial BTES temperature was set to 30°C to avoid financially infeasible solutions caused by a too long initial transient. A fixed temperature difference ΔT_{eq}= 10 K was set between the heat transfer fluid and heat source/sink for heat pump/chiller COP calculation of Eqs. 6 and 7. Table 2 shows the specific costs assumed for the heat generation systems.

Tab. 2 – Capital cost and maximum size considered for solar collectors, heat pumps and chillers.

Parameter	λ	Max. size
Solar collectors	500 €/m^2	10^4 m^2
Heat pumps	576 €/kW$_t$	3300 kW$_t$
Chillers	576 €/kW$_t$	975 kW$_t$

Two supply temperature levels were considered for the district heating network: 65°C and 40°C. The latter implies that all heat emission systems in the campus are replaced by low-temperature ones (e.g. low-temperature radiators and radiant floors), but the heating demand remains unchanged. The cooling network operates with a supply temperature of 6°C.

Assessment of the optimal solutions

A range of CO_2 prices from 50 €/t to 450 €/t was tested. As a reference, the lower limit is approximately the current EU carbon price [17], while direct extraction of CO_2 from the atmosphere is estimated to cost between 110€/t and 280€/t [18]. Both the environmental and economic parts of the objective function, i.e. annual CO_2 emissions and costs, were compared to a Baseline setup. This baseline setup consisted of a thermal network with an air-source heat pump for heating and an air-source chiller for cooling (no BTES, heat pump and chiller connected to it, or solar thermal collectors).

4. Results

Fig. 3 shows optimal design parameters, such as the volume of the BTES, the nominal heating and cooling capacity of the ground-source and air-source heat pumps and chillers (summed), and the area of the solar thermal collectors. The graphs show how different CO_2 prices influence the optimal design of the system for the two temperature levels of the district heating network. While, as expected, the size of the heat pumps and chillers does not change with the temperature levels of the district heating network (only adding solar generation can reduce the peak heating demand), the BTES volume and the surface area of the solar collectors do. It can be noted that both the BTES and the solar field increase their size with increasing CO_2 price, and that a higher-temperature network generally requires a higher BTES volume to operate optimally. This choice is linked to the optimal operation of the system, which will be discussed later in this Section. The case study is the Empa campus in Switzerland, which features a heating-dominated climate.

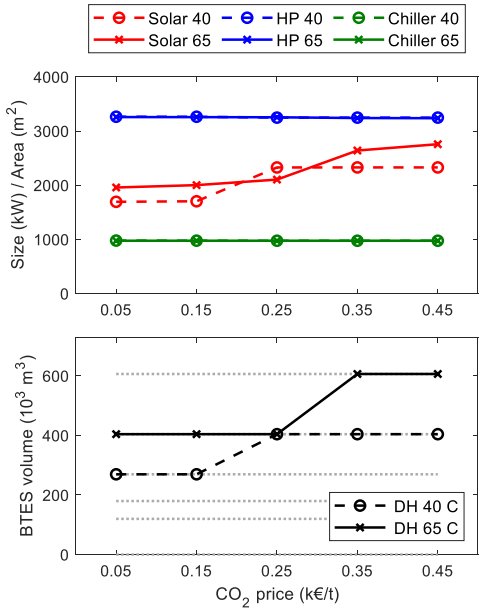

Fig. 3 - Effect of CO_2 price on key design parameters.

Therefore, the solar collectors contribute to filling the mismatch between the heat extracted from the ground during the heating season and the heat rejected into the ground during the cooling season, as shown in Fig. 4 (top) for the 65°C thermal network. The air source heat pump compensates for the remainder of the missing energy that BTES cannot provide in winter. The lower plot in Fig. 4 shows that the contribution of the air source heat pump is more significant (26%) at low CO_2 prices compared to higher ones (11%), which is clearly due to the smaller size of the seasonal thermal storage (see Fig. 3).

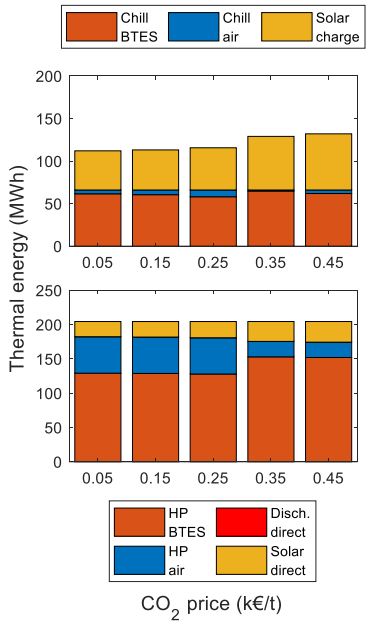

Fig. 4 - Effect of CO_2 price on the annual heating and cooling supply mix in the 65°C temperature network. Cooling operation (top), heating operation (bottom).

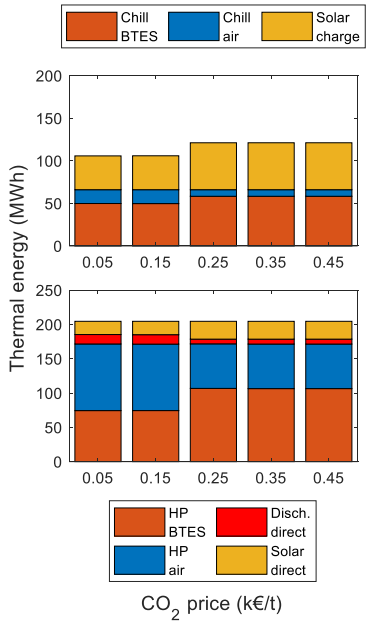

Fig. 5 - Effect of CO_2 price on the annual heating and cooling supply mix in the 40°C temperature network. Cooling operation (top), heating operation (bottom).

When the heat is supplied at 40°C in the district heating network, the relative contribution of the air source heat pump during the heating season is more significant, and ranges from 32% to 47% of the heating demand depending on the CO_2 price. Similarly to the previous higher-temperature network case, this range is due to the different optimal sizes of the BTES at the different CO_2 prices. In this case, the BTES is charged at a temperature high enough to allow a direct discharge of the heat (i.e. without a heat pump) from the BTES in Autumn, as shown by the red portions of the bars in Fig. 5 and in the upper temporal plot in Fig. 6.

Fig. 6 shows the optimal operation of the system at both temperature levels –by way of example of the identified optimal solution at a CO_2 price of 0.15 k€/t. In the upper chart, it can be seen that the average BTES temperature profile exceeds the network supply temperature (40°C), thus allowing part of the heating demand to be covered by direct BTES discharge in Autumn, which cannot occur in the high-temperature case. In the bottom chart in Fig. 6 the peak temperature barely reaches 40°C. This is not a trivial result because the optimizer could also opt for different decisions, such as a higher temperature swing of the seasonal thermal storage. The maximum temperature is a combination of the initial storage temperature and of the seasonal temperature swing. The first decision variable always reaches the upper bound, which was set at 30°C to limit the duration of the initial transient to heat the BTES (not considered in this study). The peak storage temperature in summer increases with decreasing CO_2 price, driven by the low BTES volume, but is always lower than 42.3°C. This occurs because the maximum thermal energy that can be extracted from the BTES during the heating season is constrained by its maximum heat transfer rate, which in turn depends on the volume of the storage. Therefore, the same amount of heat exchanged with a smaller BTES does not necessarily lead to a higher temperature swing. The absence of fossil-fuelled backup generators forces the air source heat pump to cover most of the remaining heating demand, including the peaks occurring in the coldest part of the winter, when the efficiency is lower and heating demand larger. In the low-temperature network, part of the heating demand is supplied by directly discharging the BTES. However, this occurs in Autumn only, when the thermal storage is almost fully charged and the heat demand is rather low (red area). In this period the CO_2 intensity is also relatively low and the outdoor air temperature mild, i.e. when the air source heat pump would have the lowest economic and environmental impact. However, the only way to increase the share of heat directly supplied from the BTES would be either to have an even lower network supply temperature or to increase the solar collector area. Therefore, the limited amount of direct storage discharge can be interpreted as an optimal trade-off between the increased investment cost needed to increase the size of the solar collector field and the reduced running costs due to avoided heat pump operation.

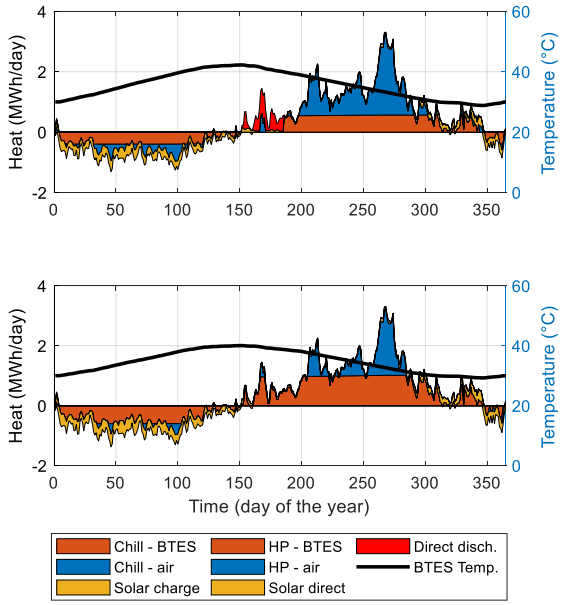

Fig. 6 - Optimal operation of the system for 40°C (top) and 65°C thermal networks (bottom).

As far as the comparison between the two district heating temperature levels is concerned, Fig. 7 shows that the solutions with the low-temperature network (black square dots) are always better than those with the high-temperature network (red squared dots), both from economic and environmental standpoints. This is mainly due to the higher COP of both the ground and air-source heat pumps in the low-temperature network, which reduces the electricity consumption to meet the same heating demand, thereby improving both indicators. The optimal solutions led to a reduction in CO_2 emissions compared to the baseline system in the range between 33.0-43.1% and a change in costs, excluding those related to CO_2 emissions, of approximately 3.2% less to 0.4% more, depending on CO_2 tariff and heating supply temperature.

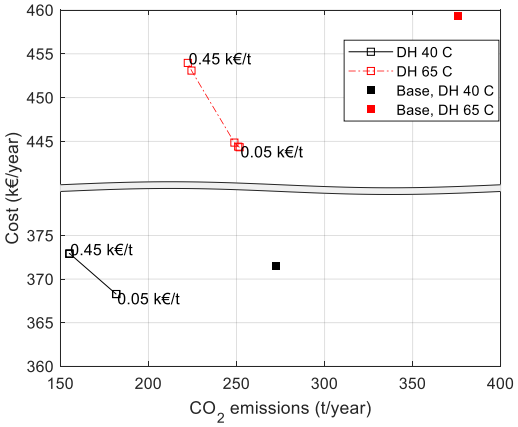

Fig. 7 – Economic vs environmental cost of the optimal solutions.

Including the cost of the CO_2 emissions as well, the optimal design of the energy system at 40°C could achieve a reduction in the range from 2% (in the case of the lowest CO_2 price) to 10.4% (in the case of the highest CO_2 price). The optimal design of the energy system at 65°C could achieve a slightly larger reduction compared to the baseline system, ranging from 4.4% to 11.8%

5. Conclusions

This paper presented a design optimization methodology for a district heating and cooling energy system integrating a Borehole Thermal Energy Storage (BTES) that considers the temperature-dependent operational implication of the BTES in conjunction with the rest of the energy system. In particular, the implications of a lower or higher heating network temperature on the optimal system design and its possibility to directly discharge the storage were studied. This methodology was applied to a case study district heating and cooling system, located in a heating-dominated climate. It was assumed that the district heating and cooling demand could be met either by an air-source heat pump and chiller, or by a BTES-connected heat pump and chiller, enabling seasonal storage of the waste heat. Solar thermal generation could also be integrated to compensate for the unbalance between cooling and heating demands. Two heating network temperatures (40 and 65°C) were studied. The optimization results showed that, for the case study system considered: i) it is always beneficial to have seasonal storage with integrated solar thermal generation, increasing in size with an increase in CO_2 price, ii) the BTES was operated at the highest initial temperature allowed, to increase heat pump efficiency during discharge and reduce CO_2 emission when the CO_2 intensity is the highest and iii) direct discharge was employed with the lower heating network temperature, but in a limited amount. This outcome is particularly interesting, as the BTES can only be discharged at the beginning of the heating season, when the BTES temperature is the highest but the CO_2 intensity not as much. Furthermore, the highest point of the BTES temperature swing is limited by the limited maximum heat transfer rate associated with the BTES size, as the borehole density is assumed to remain constant with the different BTES sizes considered.

6. Acknowledgement

The authors would like to acknowledge the financial support of the Swiss Federal Office of Energy SFOE through the SWEET DeCarbCH program and of the Swiss National Science Foundation SNSF through the Sinergia SOTES project.

7. References

[1] Sibbitt B, McClenahan D, Djebbar R, Thornton J, Wong B, Carriere J, et al. The Performance of a High Solar Fraction Seasonal Storage District Heating System – Five Years of Operation. Energy Procedia 2012;30:856–65. https://doi.org/10.1016/J.EGYPRO.2012.11.097.

[2] Laboratory U of W--MSE, Klein SA. TRNSYS, a transient system simulation program. Solar Energy Laborataory, University of Wisconsin--Madison; 1979.

[3] Shah SK, Aye L, Rismanchi B. Seasonal thermal energy storage system for cold climate zones: A review of recent developments. Renew Sustain Energy Rev 2018;97:38–49. https://doi.org/10.1016/j.rser.2018.08.025.

[4] Antoniadis CN, Martinopoulos G. Optimization of a building integrated solar thermal system with seasonal storage using TRNSYS. Renew Energy 2019;137:56–66. https://doi.org/10.1016/j.renene.2018.03.074.

[5] Prasanna A, Dorer V, Vetterli N. Optimisation of a district energy system with a low temperature network. Energy 2017;137:632–48. https://doi.org/10.1016/j.energy.2017.03.137.

[6] Gabrielli P, Gazzani M, Martelli E, Mazzotti M. Optimal design of multi-energy systems with seasonal storage. Appl Energy 2018;219:408–24. https://doi.org/https://doi.org/10.1016/j.apenergy.2017.07.142.

[7] Wirtz M, Kivilip L, Remmen P, Müller D. 5th Generation District Heating: A novel design approach based on mathematical optimization. Appl Energy 2020;260:114158. https://doi.org/10.1016/j.apenergy.2019.114158.

[8] Fiorentini M, Baldini L. Control-oriented modelling and operational optimization of a borehole thermal energy storage. Appl Therm Eng 2021:117518. https://doi.org/10.1016/J.APPLTHERMALENG.2021.117518.

[9] Miglani S, Orehounig K, Carmeliet J. Integrating a thermal model of ground source heat pumps and solar regeneration within building energy system optimization. Appl Energy 2018;218:78–94. https://doi.org/10.1016/J.APENERGY.2018.02.173.

[10] Fiorentini M, Heer P, Baldini L. Design optimization of a borehole seasonal thermal energy storage in a district heating and cooling system. Manuscript submitted for publication.

[11] Gurobi. Gurobi Solver. https://www.gurobi.com/products/gurobi-optimizer/ (accessed November 10, 2020).

[12] Hellström G. Ground heat storage: Thermal analyses of duct storage systems. Lund Univ 1991:310.

[13] Lofberg J. YALMIP : a toolbox for modeling and optimization in MATLAB. 2004 IEEE Int. Conf. Robot. Autom. (IEEE Cat. No.04CH37508), 2004, p. 284–9. https://doi.org/10.1109/CACSD.2004.1393890.

[14] Lawrie L, Drury C. Development of Global Typical Meteorological Years (TMYx) 2019. http://climate.onebuilding.org (accessed June 3, 2021).

[15] electricitymap https://www.electricitymap.org/map (accessed November 2, 2020).

[16] Luo J, Rohn J, Bayer M, Priess A. Thermal performance and economic evaluation of double U-tube borehole heat exchanger with three different borehole diameters. Energy Build 2013;67:217–24. https://doi.org/10.1016/j.enbuild.2013.08.030.

[17] EMBER Daily EU ETS carbon price n.d. https://ember-climate.org/data/carbon-price-viewer/ (accessed April 30, 2021).

[18] IEA. Levelised cost of CO2 capture by sector and initial CO2 concentration 2019. https://www.iea.org/data-and-statistics/charts/levelised-cost-of-co2-capture-by-sector-and-initial-co2-concentration-2019.